Clay minerals as alteration products in basaltic volcaniclastic deposits of La Palma (Canary Islands, Spain)

E. García-Romero[a,*], J. Vegas[b,c], J.L. Baldonedo[d], R. Marfil[c]

[a]*Departamento Cristalografía y Mineralogía, Facultad C.C. Geológicas, UCM, 28040 Madrid, Spain*
[b]*Departamento Geodinámica, Facultad C.C. Geológicas, UCM, 28040 Madrid, Spain*
[c]*Departamento Petrología y Geoquímica, Facultad C.C. Geológicas, UCM, 28040 Madrid, Spain*
[d]*Centro de Microscopía Electrónica Luis Bru, UCM, 28040 Madrid, Spain*

Abstract

Clay minerals from several volcaniclastic environments including pyroclastic (tuffs), epiclastic (lacustrine, alluvial terraces, marine fan delta) and unconformity-related paleosols in La Palma (Canary Islands) were studied by XRD, SEM, TEM, HRTEM imaging and AEM. Clay minerals and their assemblages allowed us to distinguish between primary volcaniclastic basaltic material produced directly by pyroclastic eruptions and epiclastic volcaniclastic material derived from erosion of pre-existing volcanic rocks. The clay fractions consist mainly of smectite with minor chlorite, mica, chlorite-smectite mixed-layers and talc.

Phyllosilicates of the epiclastic units display wider compositional variations owing to wide variations in the mineralogical and chemical composition of the parent material. Most of the phyllosilicates (mica, corrensite, talc and chlorite) are inherited minerals derived from the erosion of the Basement Complex Unit, which had undergone hydrothermal alteration. Smectites of the epiclastic units are saponite and beidellite–montmorillonite derived from the hydrothermal Basement Complex Unit and from volcanic materials altered in the sedimentary environment. Conversely, clay minerals of unconformity-related paleosols are dominated by smectite composed of variable mixtures of saponite and beidellite, which were formed by pedogenetic processes with later hydrothermal influence. The mineralogical association in the pyroclastic unit is dominated by hydrothermally formed smectite (beidellite–montmorillonite), zeolites and calcite. This paper contributes to the differentiation between pyroclastic and epiclastic volcaniclastic rocks of several depositional settings in a basaltic volcanic complex by their clay minerals characterization.

Keywords: Smectite; Alteration processes; Basaltic volcanism; Volcaniclastic deposits; Quaternary; Canary Islands

1. Introduction

Clay minerals in volcanic environments are widely distributed over the Earth's surface as products of different processes such as hydrothermal

* Corresponding author. Tel.: +34 913944880; fax: +34 913944872.
E-mail address: mromero@geo.ucm.es (E. García-Romero).

alteration and chemical weathering of volcanic detritus, which result from rock–water–gas interactions. Recognition of the origin is often difficult due to simultaneous action and overlapping of processes. Today, criteria for distinguishing these processes are under discussion and several reports have described the formation of clay minerals from volcanic rocks. For example, Pevear et al. (1982), Mizota and Faure (1998), Shau and Peacor (1992), Christidis et al. (1995), Amouric et al. (2000), Cuevas et al. (2001), etc., suggest a hydrothermal origin for the genesis of smectites in volcanic deposits. On the other hand, Aoudjit et al. (1995), Ece et al. (1999), Minato (2000) and others describe clay minerals formed by chemical weathering of volcanic debris. Moreover, Grauby et al. (1994), Roberson et al. (1999), Kloprogge et al. (1999), Huertas et al. (2000), Drief et al. (2001), Ramirez et al. (1998), Fiore et al. (2001) and others, show examples of clay minerals synthesized in the laboratory.

Several studies based on different methods have focused on secondary clay minerals in low-temperature (<100 °C) altered submarine basalts (e.g. Shau and Peacor, 1992; Schiffman and Staudigel, 1994; Laverne et al., 1996; Alt, 1999). Roberson et al. (1999) stated that the alteration of basalts associated with hydrothermal fluids provides excellent "natural laboratories" for the study of alteration products with fine grained phyllosilicates being the most characteristic products of this process.

Previous studies on volcanic rocks in La Palma Island (Hernández-Pacheco and Fernández Santín, 1974; De la Nuez, 1983) have shown that the Basement Complex unit has suffered hydrothermal alteration processes. Hydrothermal fluids gave rise to the propylitisation of both the submarine volcanic sequence and the plutonic rocks of this Unit. According to these authors, transformations occurred at depths of 1.5–2.0 km and temperatures between 400 and 500 °C, giving rise to albite, epidote, chlorite, calcite and zeolites. Similarly, Schiffman and Staudigel (1994, 1995) proposed a hydrothermal metamorphism of the Basement Complex Unit, characterized by a relatively complete low-pressure–high temperature facies series encompassing the zeolite, prehnite–pumpellyite and greenschist facies. These mineral zonations imply metamorphic gradients of 200–300 °C km^{-1}. Vegas et al. (1999a,b) undertook a preliminary study on the transformation and neoformation of clay minerals from volcaniclastic deposits of the La Palma Island.

The aim of this paper is to use the mineralogical and geochemical characterization of clay minerals which result from the alteration of basaltic volcaniclastic rocks in order to distinguish their origin that varies from sedimentary, to early diagenetic and hydrothermal. Emphasis is also made on linking clay mineral composition to variations in the depositional environments (lacustrine, paleosols, alluvial terraces, marine fan delta and tuffs). Differentiation of the volcaniclastic units of the Caldera de Taburiente and Barranco de las Angustias areas is particularly difficult because the rocks are mainly basaltic. The relationship between smectite, the principal alteration mineral, and other associated minerals is discussed. The influence that certain depositional environments exert on the clay mineral assemblages is also assessed.

2. Geological and sedimentological setting

The Canary Islands are located off the northwest coast of Africa. These islands were formed on a passive margin by predominantly alkaline intraplate volcanism during the last 30 Ma (Carracedo et al., 1999). The Canary Islands have been widely studied and there are several hypotheses regarding their genesis reviewed in Araña and Ortiz (1991): the volcanism as related to the formation of a rift, plate displacement over a hot spot, a propagating fracture model or tectonic processes (vertical faults) under the influence of Alpine tectonics having an African or Atlantic connection.

La Palma is the westernmost island of the Canary Islands archipelago (Fig. 1A). It has an area of 730 km^2 and a maximum altitude of 2462 m above sea level. Large differences in altitude favoured the development of steep slopes and a highly entrenched network of barrancos. The island resulted from several volcanic episodes that started in the Miocene with the formation of a seamount which was subsequently affected by several dyke intrusion cycles giving rise to the so-called Basement Complex Unit. This basement underwent hydrothermal alteration (Hernández-Pacheco, 1971; De la Nuez, 1983; Schiffman and Staudigel, 1994,

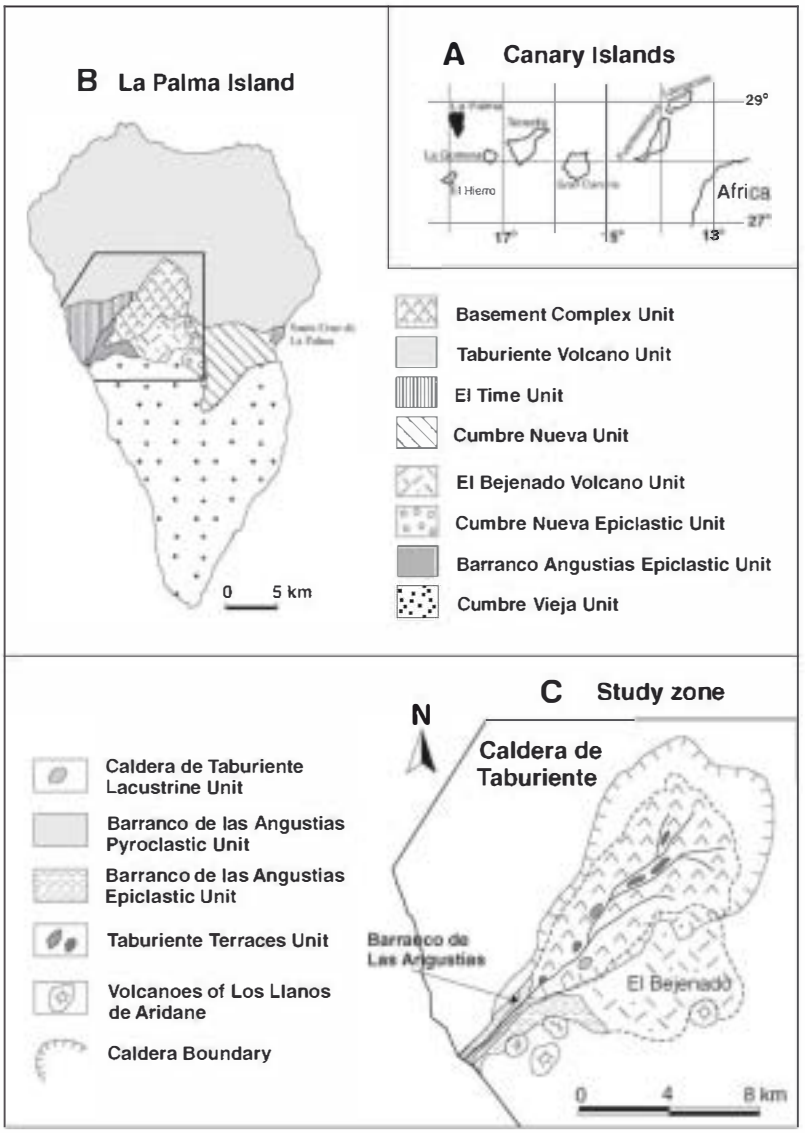

Fig. 1. (A) The Canary Islands archipelago with La Palma Island in black. (B) Sketch of the island of La Palma showing main geological units and features referred to in the text (according to Hernández-Pacheco, 1971; De la Nuez, 1983). (C) Simplified geological sketch of the study site (according to Vegas et al., 1999b).

1995). This main geological unit, the Basement Complex is separated from the subaerial lavas of the northern Taburiente Volcano by an erosive unconformity where several thin paleosols can be found (Vegas et al., 1999b). During the subaerial episodes, volcanic activity progressed toward the south and three main volcanic units were formed. The largest of these is the Taburiente Volcano in the north of the island, followed by the Cumbre Nueva in the central zone and the Cumbre Vieja top in the south (Fig. 1B) where recent volcanic activity is concentrated.

La Palma is the second-youngest island of the Archipelago. Geochronology estimates its age in the range of 2.0 to 0.77 Ma (Taburiente), and 0.81 to 0.69 Ma (Cumbre Nueva). The island is covered at its

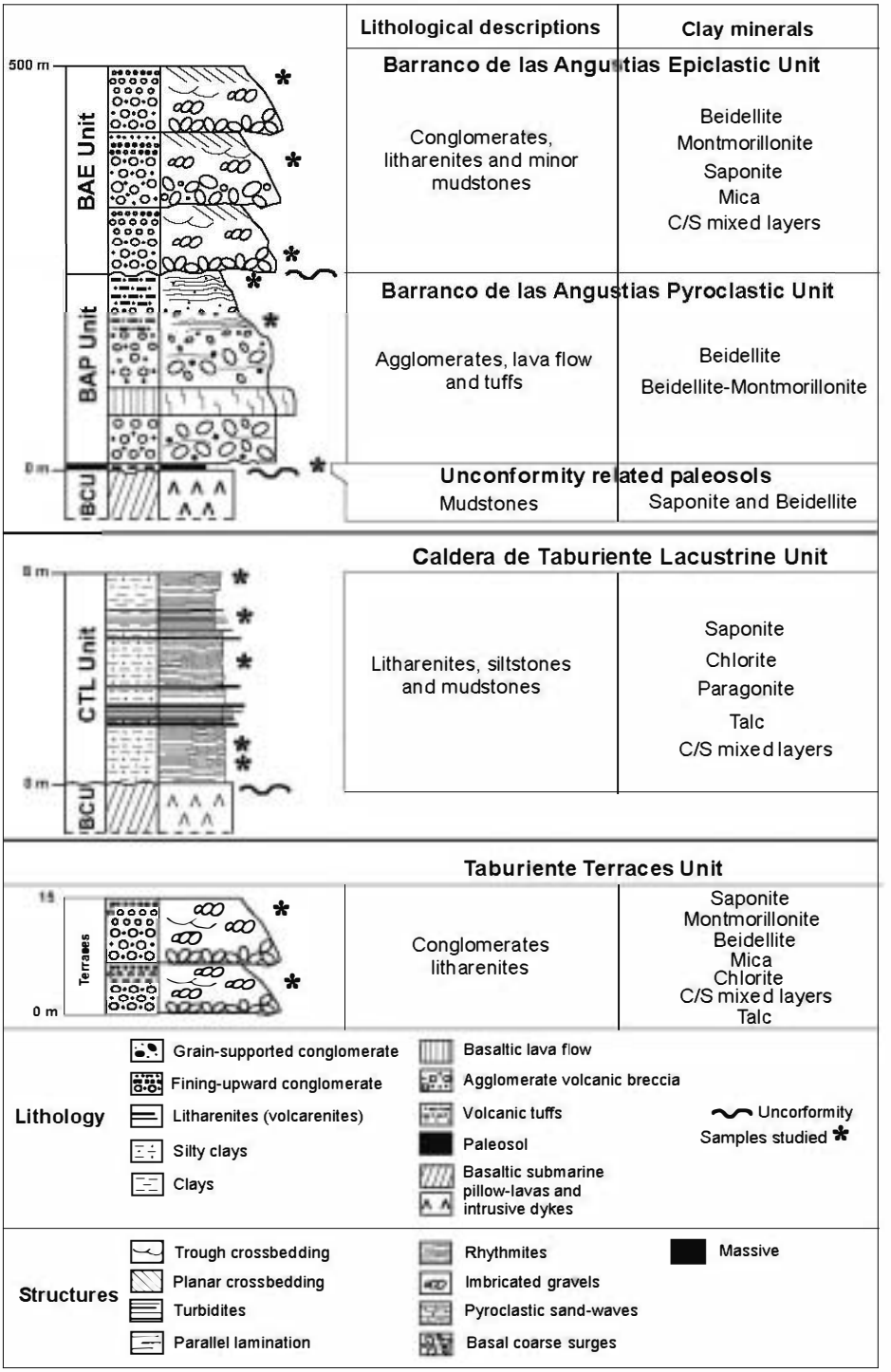

Fig. 2. Stratigraphic sections of the different volcaniclastic units referred to in the text.

southern end by the most recent volcanic unit (Cumbre Vieja), dated at 0.62 Ma to contemporary (Abdel-Monem et al., 1972; Feraud, 1981; Staudigel et al., 1986; Ancochea et al., 1994; Carracedo et al., 1999).

The present study is focused on the Caldera de Taburiente, a 15 km-long and 6 km-wide depression with bounding cliffs on most sides and a deeply dissected floor. Erosive episodes dominated during the later stages, during which a drainage network developed, converging in the Barranco de las Angustias and flowing out into the Atlantic Ocean at the island's west coast (Fig. 1C). In this context there are multiple outcrops of volcaniclastic rocks related to both volcanic and erosive-sedimentation processes. Based on a detailed study of these volcaniclastic deposits, depositional facies were defined and the different lithostratigraphical units were characterized (Vegas et al., 1999b) as described below (Fig. 2). The volcaniclastic rocks examined can be subdivided into two genetic groups (Fisher and Schmincke, 1984; Cas and Wright, 1987): (i) epiclastic sediments derived from fragments of pre-existing volcanic rocks; (ii) pyroclastic deposits composed of clastic fragments, directly derived from a volcanic eruption.

2.1. Epiclastic units

2.1.1. Caldera de Taburiente lacustrine unit (CTL Unit)

This unit is composed of silt and clays, with a minor proportion of litharenites (volcarenites) and conglomerates that define a facies of turbidites and clays deposited in a *lacustrine* environment. The macroflora fossil record suggests an age of lower–middle Pleistocene (Álvarez-Ramis et al., 2000).

2.1.2. Barranco de las Angustias epiclastic unit (BAE Unit)

This unit comprises several detrital deposits. The most abundant are formed of conglomerates, litharenites and minor mudstones. The main facies are debris flows, sheet flood and alluvial channels developing in a marine fan delta setting of upper Pleistocene age located in the Barranco de las Angustias.

2.1.3. Taburiente terraces unit (TT Unit)

These epiclastic deposits are composed of conglomerates and volcarenites of alluvial origin derived from the various erosive episodes that occurred along the Holocene. There are a variety of terraces due to the entrenchment episodes of the drainage network in the Caldera de Taburiente.

2.2. Unconformity related paleosols

At the unconformity between the Basement Complex Unit and the Barranco de las Angustias pyroclastic unit (BAP Unit) lies a paleosol of a thickness that never exceeds 30 cm (Fig. 2). This soil developed over the Basement Complex Unit and was subsequently covered by the hydrovolcanic eruption that gave rise to the BAP Unit. The A horizon appears truncated and the B horizon is highly enriched in clay minerals.

2.3. Barranco de las Angustias pyroclastic unit (BAPU)

BAP Unit is composed of breccias, agglomerates, basaltic lava flows and tuffs derived from a hydrovolcanic eruption of late Pleistocene age which formed this unit. It is found at the base of the Barranco de las Angustias underlying the BAE Unit materials, which are separated by an erosive unconformity.

3. Analytical techniques

In total 81 samples were collected from the volcaniclastic outcrops (Fig. 2) using the stratigraphic sections described in detail by Vegas et al. (1999b). Litharenite samples were impregnated with blue-stained polymer resin, and K-feldspar and carbonates were stained for light microscopy (LM). After separating the silt fraction (2–62 μm) of mudstones and paleosols, the clay fraction (<2 μm) was obtained by settling according to Stokes' Law. Mineralogical characterization was performed by X-ray diffraction (XRD) using a SIEMENS D-5000, with Cu–Kα radiation and a graphite monochromator. The samples used were random-powder specimens, air-dried, ethylene glycolated oriented clay mineral (<2 μm) aggregates and heated (550 °C for 2 h) clay fractions.

Powders were scanned from 2° to 65° and oriented aggregates from 2° to 30° 2θ, at 0.02° 2θ/s scan speed.

Particle morphology and textural relationships were established by scanning electron microscopy (SEM). SEM observations were performed using a JEOL JSM 6400 microscope operating at 20 kV and equipped with a Link System energy dispersive X-ray microanalyser (AEM). Prior to SEM examination, freshly fractured surfaces of representative samples were air-dried and coated with Au.

Undisturbed mineral particles were subjected to high resolution transmission electronic microscopy (HRTEM). Oriented sections were prepared according to the method of Tessier (1984), which involves embedding a small sample in agar to protect it. The sample was hydrated and the water replaced by

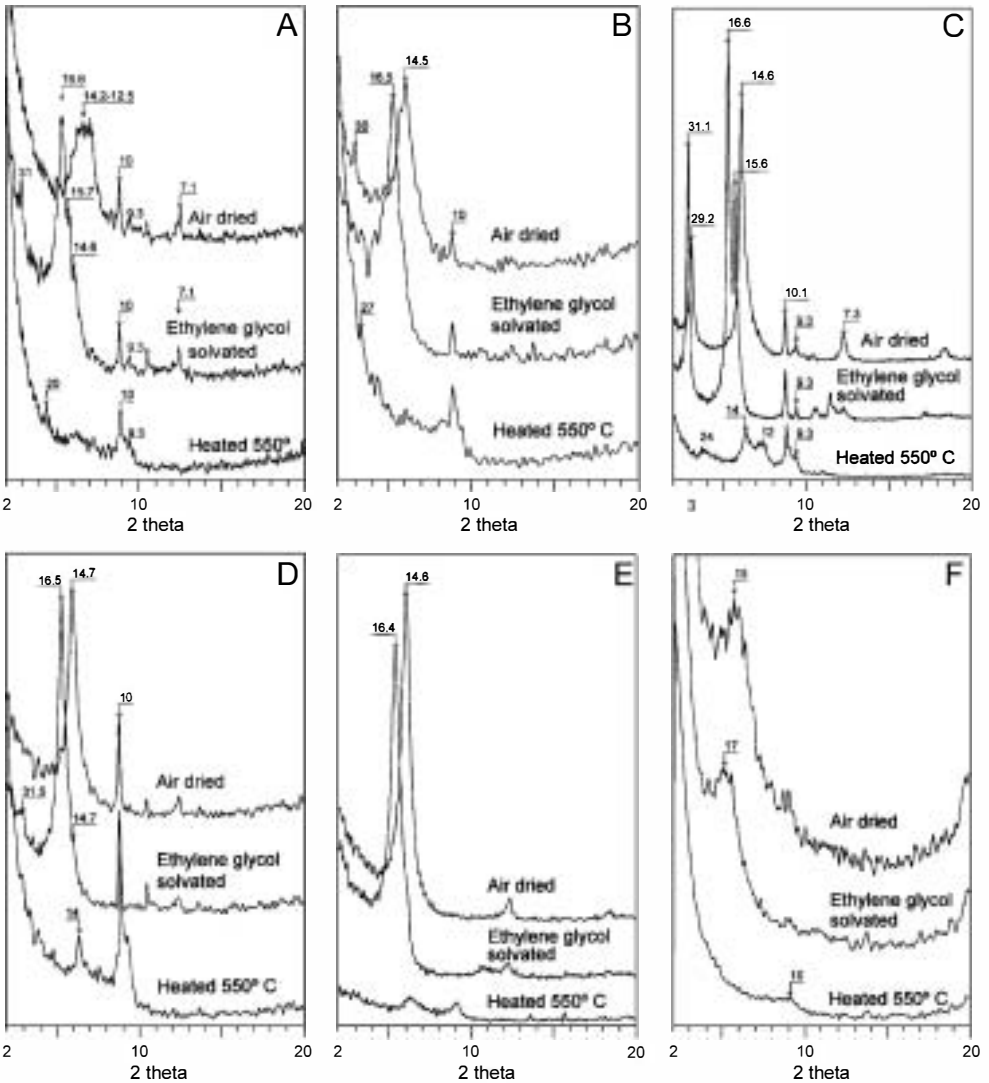

Fig. 3. XRD patterns of the oriented aggregates (air-dried, ethylene glycol solvated and 550 °C heated 2 h) of clay fraction (<2 μm). (A) Smectite, minor mica and scarce chlorite, talc and C/S mixed layer from CTL Unit. (B) Smectite, minor mica and scarce C/S mixed-layer from BAE Unit. (C) Smectite, corrensite, mica and scarce chlorite and talc from ancient terraces of the TT Unit. (D) Smectite, mica, chlorite and scarce C/S mixed layered from modern terraces of the TT Unit. (E) High cristallinity smectite from related paleosols. (F) Low cristallinity smectite from BAP Unit.

successive baths in methanol and propylene oxide before embedding in Spurr resin. After polymerization of the resin, thin sections (50 nm) were cut by ultramicrotomy. This procedure minimises dehydration during HRTEM and thus helps preserve the natural texture of the sample. Samples were examined using a JEOL 4000 EX HRTEM equipped with a double-tilt sample holder (up to a maximum of ±20°) with acceleration voltage of 400 kV, and point-to-point resolution of 0.18 nm.

Chemical composition was obtained by analytical electron microscopy (AEM) with TEM, in samples of great purity, using a JEOL 2000 FX microscope equipped with a double-tilt sample holder (up to a maximum of ±45°) at an acceleration voltage of 200 kV, with 0.5 mm zeta-axis displacement and 0.31 nm point-to-point resolution. The microscope incorporates an OXFORD ISIS energy dispersive X-ray spectrometer (136 eV resolution at 5.39 keV) and has its own software for quantitative analysis. The structural formula of 2:1 clays was calculated on the basis of 22 oxygen per unit-cell, and the 2:1:1 for 28 oxygen. All Fe present were considered as Fe^{3+}(due to the limitation of the technique), but the possible existence of Fe^{2+}should be taken into account.

4. Results

4.1. Epiclastic units

4.1.1. Caldera de Taburiente lacustrine unit (CTL Unit)

This unit is formed by litharenite and siltstone, and is mainly composed of rock fragments (RF) of alkali gabbros and low-grade basaltic pillow-lavas from the Basement Complex Unit. There is a minor proportion of RF basalts and trachybasalts from subaerial volcanism, along with pyroxene fragments. Accessory components (<3%) include olivines, amphiboles, plagioclase microlites and opaque minerals. The matrix of the litharenites is composed of plagioclase, glass and clay minerals. Detrital grains are sub-rounded due to the transport processes.

The clay fraction comprises smectites, minor mica and scarce chlorite, talc and C/S mixed-layers. Fig. 3A shows the XRD pattern representative of these samples. The air-dried pattern exhibits a broad band between 14.5 and 12.5 Å which includes smectite and chlorite, and possibly mixed-layer reflections. This band can be separated into several peaks under ethylene glycol solvated conditions. The most important reflection (16.6 Å) corresponds to smectite, the

Table 1
Chemical composition and crystallochemical formulae of the phyllosilicates from the CTL Unit

	Illites					Chlorites				Smectites				
SiO_2	51.91	51.53	43.97	46.97	56.97	50.36	36.65	38.52	38.70	35.22	52.24	64.16	52.44	53.85
TiO_2	0.34		0.58	1.14		0.27		0.13				0.16		
Al_2O_3	20.05	15.41	18.01	16.73	12.43	13.39	15.91	16.45	16.53	15.11	11.71	3.77	15.33	16.46
Fe_2O_3	12.92	22.16	12.09	13.46	10.24	16.88	28.77	22.68	22.79	21.70	5.53	6.04	17.14	13.00
MgO	7.47	14.23	17.24	14.05	25.43	12.30	17.70	21.27	21.37	20.94	28.86	25.37	13.93	12.95
CaO	0.57	0.34	1.53	2.56	1.34	1.23	0.97	0.56	0.62	0.29	0.66	0.31	0.78	1.50
Na_2O	5.85	5.73	6.30	4.77	5.97	4.94								
K_2O	0.88	0.59	0.28	0.32		0.62		0.63		0.38		0.19	0.38	2.24
Si	6.58	6.14	5.73	6.08	6.48	6.52	6.36	6.55	6.57	6.36	6.54	7.81	6.61	6.77
Al(IV)	1.42	1.86	2.27	1.92	1.52	1.48	1.64	1.45	1.43	1.64	1.46	0.19	1.39	1.23
Al(VI)	1.59	0.31	0.50	0.64	0.15	0.57	1.61	1.75	1.88	1.58	0.27	0.35	0.90	1.22
Ti	0.03		0.06	0.11		0.03		0.17				0.01		
Fe3+	1.32	2.12	1.26	1.40	0.94	1.75	3.75	2.90	2.91	3.14	0.56	0.59	1.73	1.31
Mg	1.41	2.53	3.35	2.71	4.31	2.37	4.58	5.39	5.41	5.63	5.39	4.60	2.62	2.43
Ca	0.08	0.04	0.21	0.35	0.16	0.17	0.18	0.10	0.13	0.06	0.09	0.04	0.11	0.20
Na	1.44	1.32	1.59	1.20	1.32	1.24								
K	0.14	0.09	0.05	0.05		0.10		0.14		0.09		0.03	0.06	0.36
Σ oct.	4.35	4.96	5.17	4.86	5.40	4.72	9.95	10.21	10.20	10.36	6.22	5.55	5.25	4.96

The structural formula of 2:1 clays was calculated on the basis of 22 oxygen per unit-cell, and the 2:1:1 for 28 oxygen. All Fe present were considered as Fe^{3+}(more abundant in the surface environment) but the possible existence of Fe^{2+}should be taken into account.

14.6 Å peak to chlorite and the 31 Å peak to mixed-layers. Likewise, mica and scarce talc are present (10 and 9.3 Å air-dried, ethylene glycol solvated and heated patterns, respectively).

Table 1 shows structural formulae for mica, chlorite and low-charge saponite phyllosilicates obtained by AEM microanalyses of isolated clay particles. It is noticeable that micas contain between 1.2 and 1.6 atoms of Na per unit cell suggesting a paragonitic composition and that they have a low charge (vermiculite charge) as consequence of weathering processes. Clay minerals of these samples plot (Figs. 4 and 5) in two different areas: very low charge trioctahedral smectites and micas.

The SEM images of the siltstones show a highly heterogeneous microfabric with subangular particles (30 to <1 μm). Pyroxene crystals remain and plagioclase microlites are partly transformed to smectites. In several cases only coatings of smectites appear (Fig. 6a,b). These coatings form bridges between grains at different stages of alteration. It is common to observe tubes related to organic matter filled with fibrous calcite cement.

From HRTEM observations the mica particles show relatively defect-free lattice fringes, with a continuous and constant 10 Å interlayer spacing. These particles show exfoliation or micro-division perpendicular to the stacking direction (Fig. 7a).

4.1.2. Barranco de las Angustias epiclastic unit (BAE Unit)

The conglomerates and sandstones of this Unit are mainly composed of rock fragments (RF), pyroxenes and plagioclases. The RF are derived from basalts and trachybasalts from the subaerial volcanism of the Taburiente Volcano, and to a lesser extent from alkali gabbros and low-grade metabasaltic pillow-lavas from the Basement Complex Unit. Accessory components (<3%) are olivine, opaque minerals and amphibole. The matrix is composed of fragments of plagioclase, glass and clay minerals. These epiclastic deposits display intergranular porosity with intercommunicat-

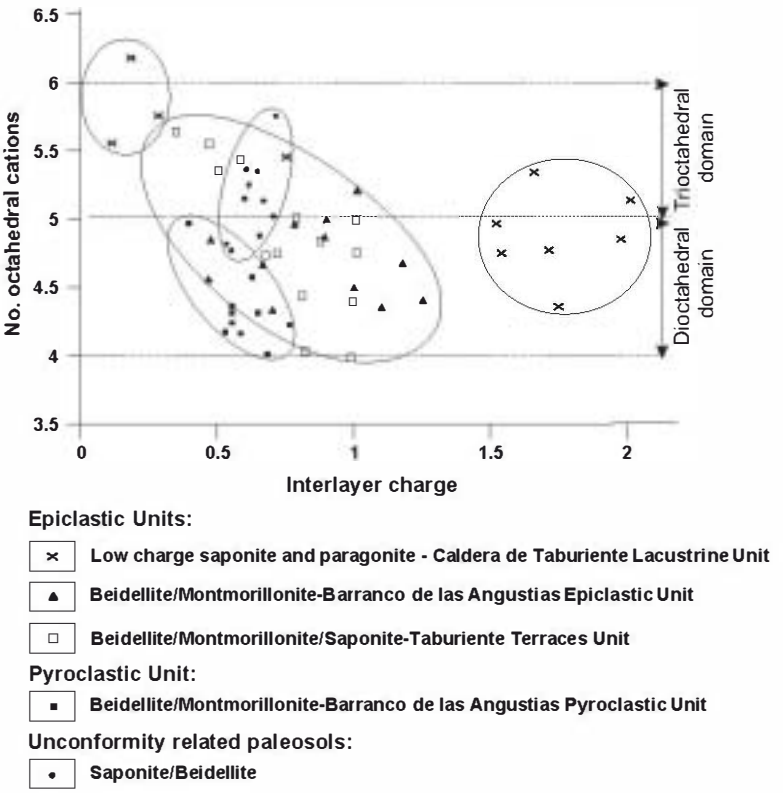

Fig. 4. Number of octahedral cations against interlayer charge plot from clay minerals of the volcaniclastic units of La Palma Island.

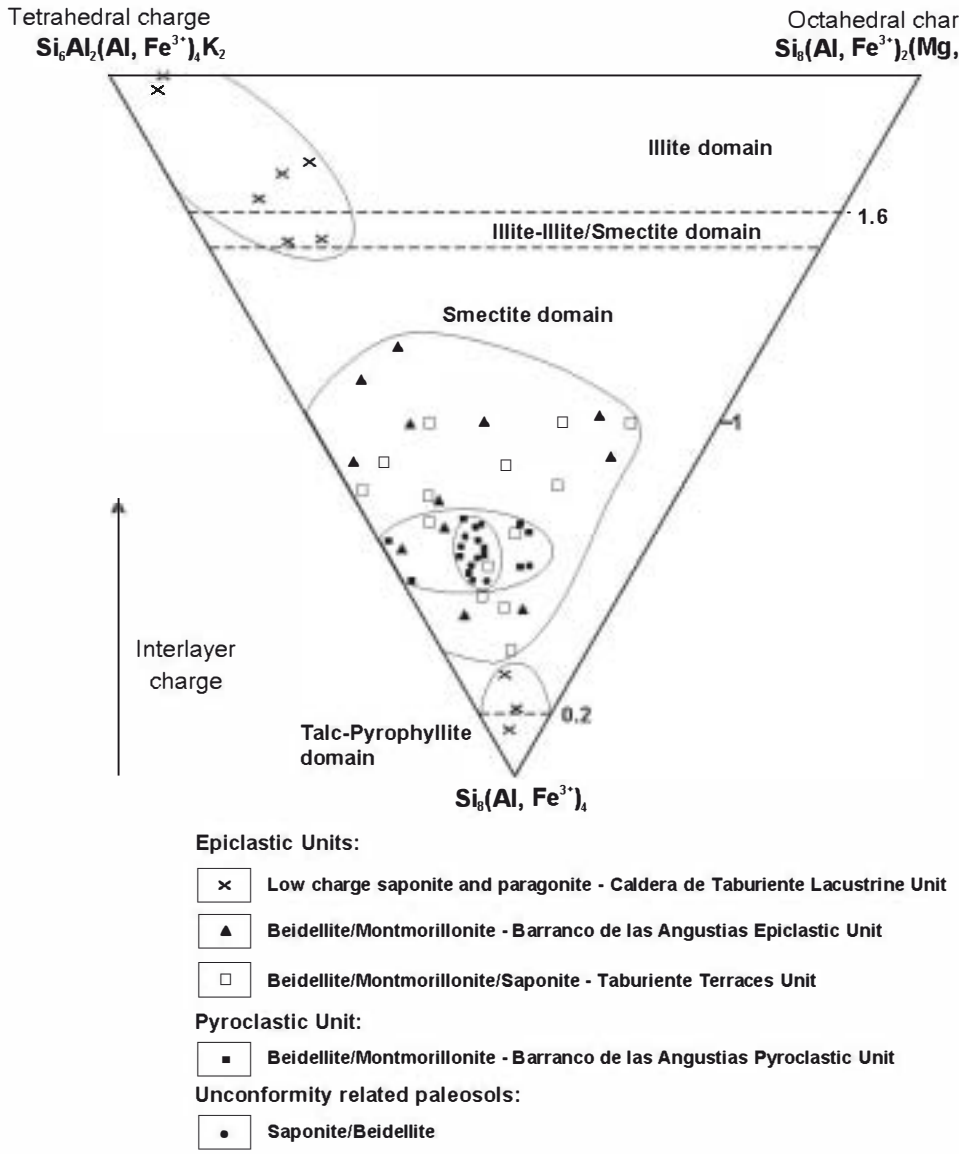

Fig. 5. Crystallochemical formulae representation after Newman and Brown (1987) from clay minerals of the volcaniclastic units of La Palma Island.

ing pores. Argillaceous coatings that act as bridges between the grains of the skeleton are frequently observed.

Phyllosilicates identified in the <2 μm fraction are smectite, minor mica and scarce C/S mixed-layers. Air-dried smectite exhibits basal spacing of 14.5 Å, which expands to 16.5 Å upon ethylene glycol solvation. The smectite fraction fully collapses to 10 Å upon heating to 550 °C. Conversely, the mica exhibits a 10 Å spacing upon successive chemical and heat treatments. XRD traces of random mixed-layer clays are observed at low angles (Fig. 3B).

The AEM analyses of smectite particles show a dioctahedral composition (Table 2 and Fig. 4). The structural formulae vary between beidellite and montmorillonite end members. These smectites have

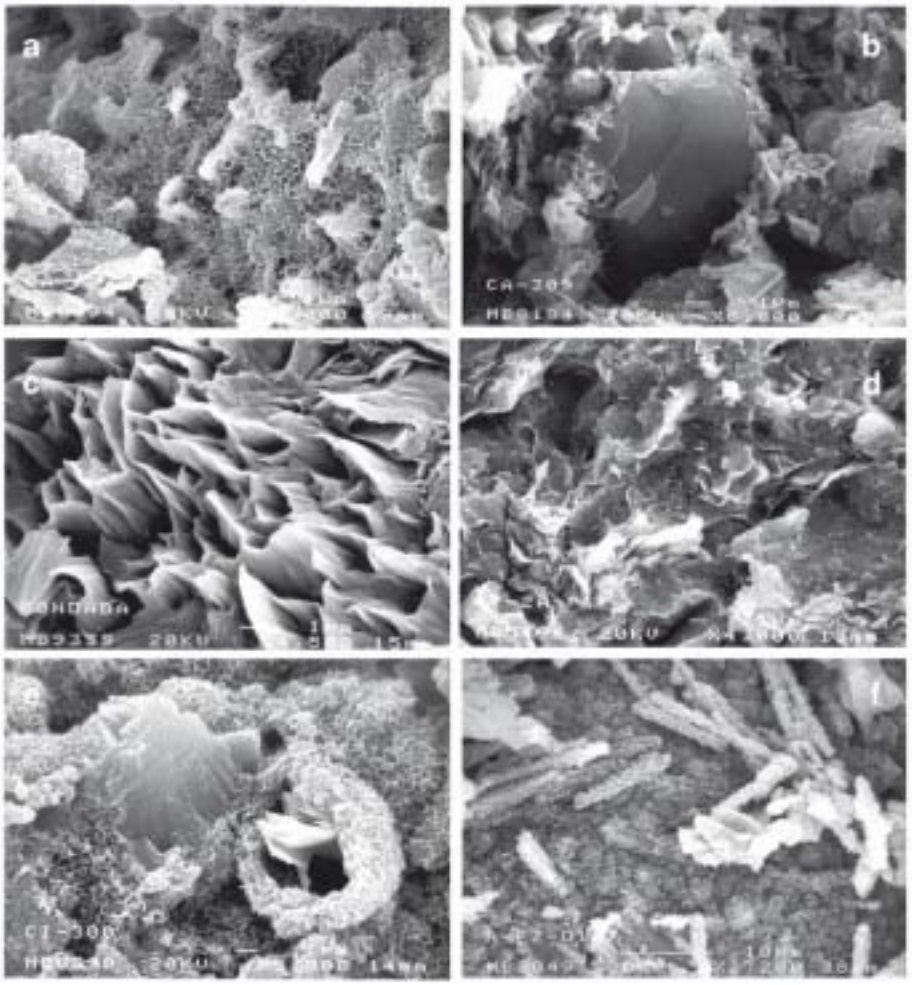

Fig. 6. SEM images of (a, b) Coatings of smectite which partly replace crystals in lacustrine sediments (CTL Unit). (c) Detailed view of mixed layers growing on the matrix of terrace conglomerates (TT Unit). (d) Irregular flocks of smectites developed on the paleosol. (e) Cornflake smectite replacing the vitric matrix and crystals in the BAP Unit. (f) Smectite coating on plagioclase microlites (BAP Unit).

continuous values between tetrahedral and octahedral charge, as shown in Fig. 5.

SEM images show smectite coatings on the RF, pyroxene crystals and other ferromagnesian components. Smectite is characterized by a well-preserved cornflake-like microfabric. Transition zones between mineral fragments and smectite may be observed; some pyroxene crystals within the coating remain unaltered. The zones not transformed to smectite are partially replaced by calcite. HRTEM images of smectite particles show anastomosing and imperfect 14 Å lattice fringe images and numerous dislocations.

4.1.3. Taburiente terraces unit (TT Unit)

The conglomerates of this Unit contain the highest compositional clay mineral variability. Unaltered RF and minerals together with particles totally transformed to clay minerals are frequent. Clay minerals also have a high variability from sample to sample. Some of them have smectite, mica and scarce chlorite, talc and mixed-layers minerals. In contrast, other samples contain higher quantities of mixed layer clay minerals. Fig. 3C displays an XRD pattern for an ordered (R1) C/S mixed layered clay mineral (corrensite). The air-dried form has a rational pattern with superstructure (001) at 29.2, 14.6 and 7.3 Å. The

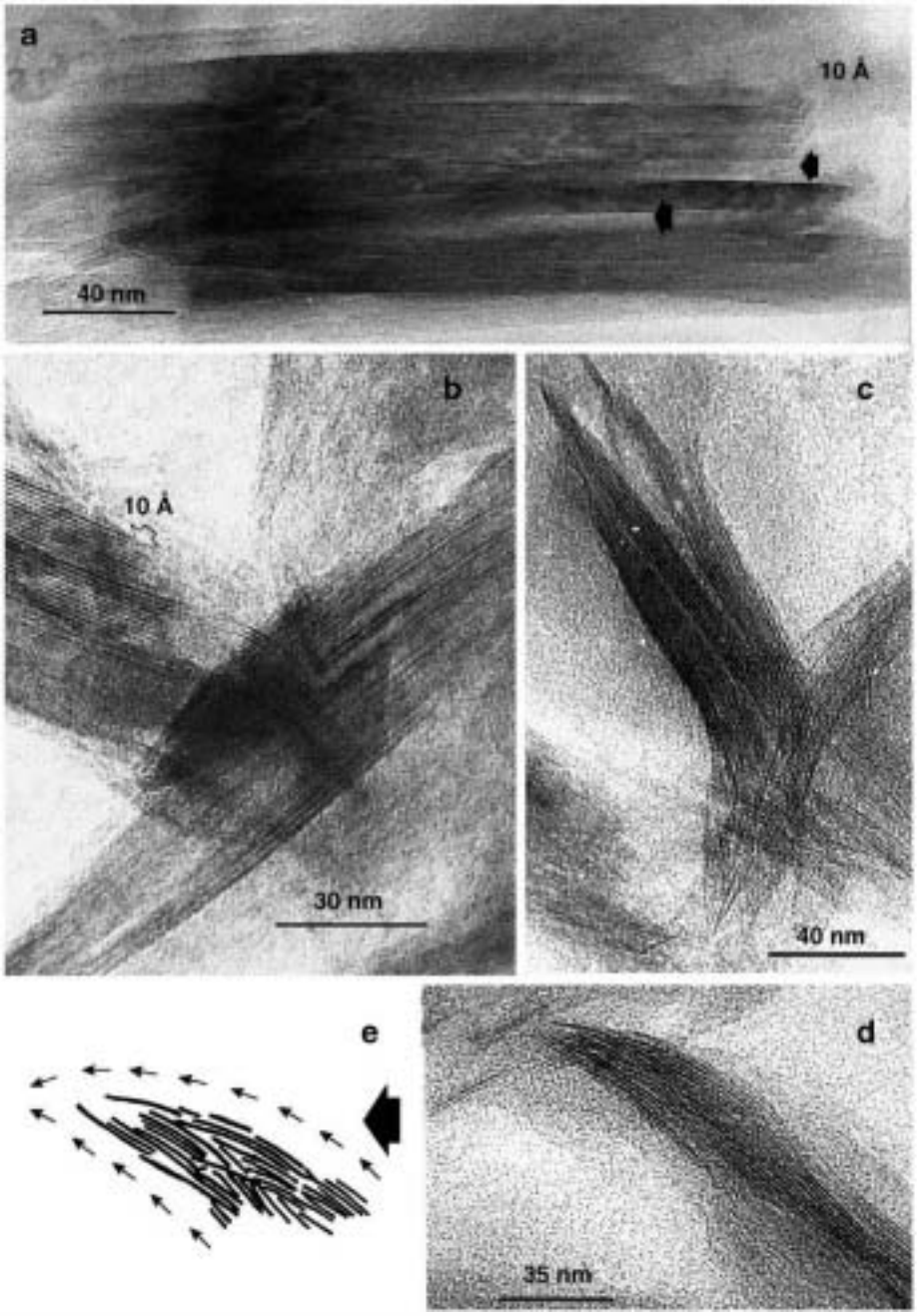

Fig. 7. HRTEM micrographs: (a) Mica particle of the TT Unit. Black arrows show exfoliation planes along which the particles break down. (b) Mica particle (10 Å) and R=1 C/S mixed layer of the TT Unit. (c, d) Anastomosing and wavy fringes on smectite particles showing a "thin brush tip" appearance from unconformity related paleosols and BAP Unit. (e) Simplified diagram illustrating this process.

ethylene glycol solvated example also produces a rational pattern, in this case the superstructure has spacing at 31.1, 15.6 and 7.8 Å. The heat-treated pattern has weak peaks at 24 and 12 Å. This sample also contains smectite with a strong reflection at 14.6 Å in the air-dried conditions, 16.6 Å in the ethylene

Table 2
Chemical composition and crystallochemical formulae of the phyllosilicates from the BAE Unit

	Smectites											
SiO_2	57.54	59.16	60.34	60.06	55.35	51.21	59.72	55.22	57.37	53.85	64.04	61.98
TiO_2	1.76	0.55		0.55	0.98	0.17	0.52	0.35	0.69		0.46	0.49
Al_2O_3	19.00	12.98	17.39	15.22	12.45	14.03	12.76	17.38	12.59	16.46	12.95	13.56
Fe_2O_3	7.32	17.88	12.07	10.04	14.96	13.27	12.25	9.22	10.33	13.00	6.94	7.48
MgO	9.26	6.62	8.52	11.15	11.99	17.46	11.03	11.34	13.70	12.95	12.14	10.29
CaO	3.73	2.17	1.68	2.12	4.13	3.60	3.72	1.63	3.32	1.50	3.29	3.66
Na2O												0.54
K_2O	1.38	0.64		0.45	0.13	0.26				2.24	0.19	
Si	7.07	7.38	7.35	7.37	6.97	6.49	7.38	7.08	7.23	6.77	7.75	7.68
Al(IV)	0.92	0.62	0.65	0.63	1.03	1.51	0.62	0.92	0.77	1.23	0.25	0.32
Al(VI)	1.84	1.30	1.86	1.58	0.83	0.59	1.24	1.72	1.11	1.22	1.60	1.67
Ti	0.16	0.05		0.05	0.09	0.02	0.05	0.03	0.06		0.04	0.05
Fe3+	0.72	1.79	1.18	0.99	1.51	1.35	1.22	0.95	1.05	1.31	0.67	0.74
Mg	1.70	1.23	1.55	2.04	2.25	3.30	2.03	2.17	2.57	2.43	2.19	1.90
Ca	0.49	0.29	0.22	0.28	0.56	0.49	0.49	0.22	0.45	0.20	0.43	0.49
Na												0.13
K	0.21	0.10		0.07	0.02	0.04				0.36	0.03	
Σ oct.	4.42	4.37	4.59	4.66	4.68	5.26	4.54	4.87	4.79	4.95	4.50	4.36

glycol and collapses at 10 Å after heat treatment. Moreover, another weak peak appears at 9.3 Å after both treatments, appropriate to talc. Reflections at 14 Å are interpreted as chlorite. XRD results in Fig. 3D have similar composition, but only scarce corrensite is present.

The variability in chemical composition (Table 3) indicates marked compositional differences between smectites. Formulae calculated from microanalyses of isolated clay particles vary between di- and trioctrahedral smectites and, montmorillonite and beidellite end members (Figs. 4 and 5).

SEM observations of these clay minerals show curved plates 7 to 15 μm in length (Fig. 6c), that possibly correspond to the mixed layer minerals identified by XRD (Fig. 3C). A small proportion of smectites with a cornflake texture filling some of the pores between these curved plates was also observed.

Table 3
Chemical composition and crystallochemical formulae of the phyllosilicates from the TT Unit

	Smectites							Chlorites									
SiO_2	60.22	64.08	59.47	54.97	49.75	60.61	59.36	50.50	53.96	41.42	53.28	53.09	43.69	47.31	41.42	40.72	37.70	36.65	47.22
TiO_2				0.96	0.21				0.62										
Al_2O_3	9.62	19.87	5.02	17.86	29.62	6.12	5.43	9.60	10.43	18.68	10.19	7.95	12.29	10.33	18.68	13.94	18.19	15.91	12.01
Fe_2O_3	23.36	7.98	15.54	13.19	13.21	17.13	16.39	20.33	21.01	23.54	18.84	18.02	24.67	23.07	23.54	22.27	27.24	28.77	21.21
MgO	3.51	3.66	15.72	10.17	2.41	13.66	15.64	12.14	6.88	13.78	14.67	18.41	15.85	16.37	14.38	12.27	16.21	17.70	18.10
CaO	2.48	3.34	3.48	2.34	2.23	2.48	3.18	2.19	2.57	0.01	2.56	1.89	1.95	2.35	1.01	1.72	0.60	0.97	0.83
Na_2O																			
K_2O	0.81	1.08	0.76	0.50	2.57			5.25	0.54	0.97	0.46	0.64	1.55	0.57	0.97				0.63
Si	7.61	7.71	7.51	6.83	6.22	7.59	7.47	6.68	7.15	5.50	6.81	6.80	7.39	7.88	7.02	7.53	6.49	6.36	7.88
Al(IV)	0.39	0.29	0.49	1.17	1.78	0.41	0.53	1.32	0.85	2.50	1.19	1.20	0.61	0.12	0.98	0.47	1.51	1.64	0.13
Al(VI)	1.05	2.54	0.26	1.46	2.60	0.50	0.28	0.18	0.79	0.44	0.35		1.85	1.92	2.75	2.57	2.18	1.61	2.23
Ti				0.09	0.02				0.06										
Fe3+	2.37	0.77	1.58	1.32	1.33	1.72	1.66	2.16	2.24	2.51	1.93	1.85	3.35	3.09	3.00	3.10	3.58	3.75	2.66
Mg	0.66	0.66	2.96	1.88	0.45	2.55	2.93	2.39	1.36	2.73	2.79	3.51	3.00	4.07	3.57	3.38	4.16	4.58	4.50
Ca	0.34	0.43	0.47	0.32	0.30	0.33	0.43	0.31	0.36	0.01	0.35	0.26	0.35	0.42	0.18	0.34	0.01	0.18	0.15
Na																			
K	0.14	0.17	0.12	0.08	0.41			0.89	0.09	0.17	0.08	0.10	0.33	0.12	0.21				0.13
Σ oct.	4.08	3.97	4.80	4.75	4.40	4.77	4.87	4.73	4.44	5.68	5.07	5.36	8.19	9.07	9.32	9.05	9.93	9.95	9.39

Table 4
Chemical composition and crystallochemical formulae of the phyllosilicates from the unconformity related paleosols

	Smectites								
SiO_2	52.13	49.94	51.31	47.50	53.87	50.11	55.78	54.00	52.81
TiO_2		0.88	0.79		1.47	1.10			
Al_2O_3	13.51	17.51	14.71	14.40	16.97	13.57	15.21	13.67	13.61
Fe_2O_3	15.69	15.77	15.56	14.02	15.51	19.66	16.45	18.08	22.35
MgO	16.32	13.33	15.34	21.08	12.70	12.98	10.53	11.59	9.29
CaO	2.32	2.23	2.10	1.91	2.17	2.44	2.04	1.97	1.91
Na_2O						0.14			
K_2O		0.34	0.19	1.08			0.50	0.69	
Si	6.59	6.32	6.49	6.09	6.58	6.42	6.72	6.83	6.73
Al(IV)	1.41	1.68	1.51	1.91	1.42	1.58	1.05	1.17	1.27
Al(VI)	0.61	0.94	0.69	0.27	1.03	0.48	1.19	0.88	0.78
Ti		0.08	0.08		0.14	0.11			
Fe3+	1.59	1.60	1.58	1.44	1.52	2.02	1.65	1.84	2.29
Mg	3.08	2.52	2.89	4.03	2.31	2.48	1.96	2.19	1.77
Ca	0.31	0.30	0.29	0.26	0.28	0.33	0.27	0.27	0.26
Na									
K		0.06	0.03	0.18		0.03	0.08	0.11	
Σ oct.	5.28	5.14	5.24	5.74	5.00	5.09	4.80	4.91	4.84

HRTEM images show that the smectites are thin crystals (2/3–20 layers thick), have a large number of dislocations, ill-defined grain edges and step-shaped lamina tips. The chlorite particles show a relatively defect-free lattice fringes, with continuous and constant 14 Å interlayer spacings, and exfoliation perpendicular to the stacking direction which shows small-sized crystals (maximum 30 layers). Mixed-layer clay minerals are formed by a regular alternation of groups of layers (Fig. 7b).

4.2. *Unconformity related paleosols*

The paleosol samples are mudstones where clay minerals (smectites) dominate with minor plagioclase, augite and olivine. XRD patterns are shown for the air-dried, ethylene glycol solvated and heated treatment of the smectite (Fig. 3E). The weak XRD pattern of these phases is noticeable suggesting a high crystallinity of these samples. The smectites have a chemical composition intermediate between Fe-rich saponites and beidellites (Table 4; Figs. 4 and 5).

The SEM observations show that smectites formed by the alteration of phenocrysts have a morphology consisting of irregular cornflake type particles with undulating edges (Fig. 6d). The pores related to organic tubes show neoformation of prismatic zeolites. In the sections examined by HRTEM, the smectites comprise crystals with many edge dislocations and their tips are step-shaped, or display a "thin brush tip" (Fig. 7c).

4.3. *Barranco de las Angustias pyroclastic unit (BAP Unit)*

This Unit is formed by tuffs (<2 mm) composed of a glassy matrix embedding different types of basaltic RF

Table 5
Chemical composition and crystallochemical formulae of the phyllosilicates from the BAP Unit

	Smectites									Glass				
SiO_2	64.72	55.70	63.77	61.16	63.52	64.07	63.03	60.82	63.3	63.54	68.58	65.06	62.98	38.35
TiO_2	0.23	0.64	1.21	1.55	1.83	1.59	1.45	1.38	1.12	1.64	2.46	1.90	2.67	0.07
Al_2O_3	19.66	16.42	20.96	22.06	18.15	19.00	20.84	24.56	22.63	18.21	11.15	0.01	17.78	12.15
Fe_2O_3	6.31	13.11	6.51	7.01	9.28	7.76	7.73	6.05	5.86	10.53	15.18	11.21	9.35	38.71
MgO	5.74	11.91	4.77	4.79	4.21	4.97	4.44	4.29	4.70	1.35	0.17	1.16	1.89	7.03
Cr_2O_3		0.31	0.24	0.24	0.41	0.35	0.27	0.25	0.25					
CaO	2.04	1.72	2.25	2.61	2.24	1.85	1.92	2.15	1.80	4.72	2.46	4.56	5.34	0.62
K_2O	0.21	0.20	0.29	0.59	0.37	0.4	0.32	0.50	0.30					3.07
Si	7.77	6.91	7.61	7.34	7.66	7.68	7.55	7.53	7.53					
Al(IV)	0.23	1.09	0.39	0.66	0.34	0.32	0.45	0.47	0.47					
Al(VI)	2.56	1.32	2.57	2.47	2.25	2.37	2.50	2.72	2.72					
Ti	0.02	0.06	0.17	0.14	0.17	0.14	0.13	0.10	0.10					
Fe3+	0.61	1.31	0.62	0.68	0.90	0.75	0.74	0.56	0.55					
Mg	1.03	2.20	0.85	0.85	0.76	0.89	0.79	0.83	0.84					
Cr		0.03	0.02	0.02	0.04	0.04	0.03	0.03	0.02					
Ca	0.26	0.23	0.29	0.34	0.29	0.24	0.25	0.23	0.23					
K	0.03	0.03	0.03	0.09	0.06	0.06	0.05	0.05	0.05					
Σ oct.	4.22	4.92	4.23	4.16	4.12	4.19	4.19	4.24	4.23					

(<10%) and pyroxenes (<5%) with angular edges. Calcite which occurs as veins replacing crystals and matrix is present, together with zeolites. These tuffs show loosely packed microfabric where clay particles of cornflake-like morphology replace both the vitreous matrix and rock fragments (Fig. 6e). The smectites form coatings over the grains (Fig. 6f). Poikilotopic calcite partially replaces the glass matrix and the rock fragments. Prismatic and radial fibres of zeolites grow into the degassing pores and over the smectite coatings. XRD patterns of these smectites revealed broad peaks that reflect low crystallinity (Fig. 3F).

Smectites have a homogeneous dioctahedral composition typical of beidellites with minor intermediate beidellite–montmorillonite (Fig. 4). The glass shows low MgO (0.17–7.03%) and high Fe_2O_3 (9.35–38.71%) content; this is also reflected in the composition of the smectites, with low MgO values (4.21–11.91%) and relatively high Fe_2O_3 (5.86–13.11%). In contrast, no Na_2O and no (or very low values) K_2O was detected in the glass, suggesting that the main interlayer cation in the smectite is Ca. The content of TiO_2 reflects the proportion of TiO_2 in the glass (Table 5).

From HRTEM observations, smectite particles are composed of packets of up to 20 layers, although groups of 2–3 layers are frequently found. The layers show scarce lateral continuity and variable spaces of 12 to 17 Å, as well as numerous dislocations (Fig. 7d,e) and "thin brush tip" type end particles.

5. Discussion

The interpretation of XRD patterns SEM, TEM and HRTEM data on the volcaniclastic deposits from La Palma Island reveals clay mineral mixtures of detrital, hydrothermal and neoformed origin. In the studied deposits, clay minerals and associated carbonate and zeolites are the result of interactions between basaltic debris and meteoric, sea water or hydrothermal fluids.

5.1. Phyllosilicates of the epiclastic units

Phyllosilicates in the epiclastic units (CTL Unit, BAE Unit and TT Unit) display the widest compositional variation (Tables 1–3) reflecting the chemical composition of their mineral precursors, which are related to different volcanic source rocks during the upper Pleistocene to Holocene (Vegas et al., 1999a,b). Two main phyllosilicate assemblages were identified in these epiclastic units. First, saponite, mica, paragonite, talc, corrensite and chlorite are inherited minerals from the hydrothermally altered rock fragments derived from the erosion of the BCU. The appearance of corrensite in low-pressure environments in a seamount series at 700–800 m depth implies paleotemperatures of 225–250 °C (Bird et al., 1984) and chlorite reflects temperatures of 275–300 °C (Schiffman and Staudigel, 1994). Random mixed-layer C/S is an intermediate product when saponite is transformed to corrensite and/or chlorite (Kristmannsdottir and Tomasson, 1978; Robinson et al., 1993). Saponite may be transformed directly into corrensite with no intermediate randomly mixed-layer C/S (Shau et al., 1990; Inoue, 1995; Beaufort et al., 1997). Saponite in the upper part of basalts in the BCU was interpreted to be formed at relatively low temperatures (20–80 °C) (Schiffman and Staudigel, 1994, 1995). The high crystallinity of smectite indicates inherited origin. Thus, the presence of saponite, corrensite and chlorite in these sedimentary units suggests that these minerals are inherited from the BCU. More abundant corrensite, chlorite and paragonite in the CTL and in the TT units are attributed to a greater influence and proximity to the BCU source rocks than in the BAE Unit.

A second assemblage includes diagenetic smectites. SEM data from the epiclastic units show the presence of smectite as replacement products of mineral grains, pore filling and grain coatings (Fig. 6a–c), which suggest primary or early diagenetic origin for the smectites in the sedimentary environment. The wide range between octahedral and tetrahedral charge in smectite reflects the varying compositions of possible protoliths (Figs. 4 and 5). Cations needed for smectite formation were derived from the abundant ferromagnesian minerals in the volcanic debris at superficial meteoric conditions. Smectites of the CTL Unit were formed in small, poorly drained, lake bottom sediments during early diagenesis of volcanic materials.

5.2. Phyllosilicates of unconformity related paleosols

Mineralogy of paleosols is homogenous, being dominated by smectite (saponite and beidellite; Table 4), which is attributed to pedogenetic processes and

subsequent hydrothermal alteration, as evidenced by the deposition of BAP Unit over this paleosol (Fig. 2). Mineral decomposition of basaltic lavas is known to continue until Mg clay minerals appear as hydrothermal alteration products (Amouric et al., 2000). Fe-saponite was the most abundant secondary phase, replacing primary minerals (olivine, pyroxene and plagioclase) or occurring as vesicle fillings. The chemical composition of the secondary phyllosilicates is not significantly influenced by the host primary phases, but rather by the pore fluids (Amouric et al., 2000).

Minerals in the paleosols were completely transformed to smectite with no intermediate phases. The mineralogical homogenization and the presence of zeolites are related to the very low-temperature hydrothermal fluids that gave rise to the smectite, which is evidenced by the absence of corrensite and chlorite in the paleosols (Bird et al., 1984; Schiffman and Staudigel, 1994, 1995).

5.3. Phyllosilicates from the Barranco de las Angustias pyroclastic unit (BAP Unit)

The mineral association of this Unit (beidellite–montmorillonite series, zeolites and calcite) indicates that the pyroclastic products have undergone hydrothermal alteration related to the hydrovolcanic eruption itself. The alteration processes include devitrification of volcanic glass, followed by the hydration and crystallization of the smectite.

Similar processes have been described by Külmel and Van Der Gaast (2000), who found hydrothermal montmorillonite, which occurs in the vicinity of water springs and faulted zones associated with zeolites on Gran Canaria island. Moreover, the occurrence of zeolites indicates hydrothermal influence in the early stages of clay mineral formation (Bargar and Beeson, 1981; Inoue, 1995; Kristmannsdottir and Tomasson, 1978).

Smectite from the BAP Unit shows very low crystallinity (Fig. 3F) because the crystals are at the first stages of their growth, and therefore the degree of structural order is still limited. HRTEM images allowed the observation of thin crystals (2–3 layers) and numerous defects (edge dislocations) (Fig. 7d) indicating that smectite particles are in the first stages of formation. The main steps of particles growth are located along the edges of the laminae. The high bonding forces (covalent bond in the octahedral sheets) and the combination of numerous edge dislocations result in "thin brush tips" ends (Fig. 7d,e). The ends observed with HRTEM probably correspond to the fibres present in the undulated margins of the smectite particles (Fig. 6e,f). The chemical composition of the smectite suggests that glass and plagioclase chemistry control the composition. SEM observations indicate the presence of authigenic phyllosilicates, zeolite and calcite that fill fractures, vesicles and replace highly reactive glass and primary minerals.

6. Conclusions

This paper demonstrates that major factors controlling clay mineral composition in volcaniclastic rocks include the source and chemistry of volcanic detritus as well as the depositional environment and early diagenetic processes. Clay minerals composition and assemblages allowed us to distinguish between volcaniclastic basaltic material produced directly by volcanic eruptions (pyroclastic) and volcaniclastic material derived from erosion of pre-existing volcanic rocks and shallow intrusive rocks (epiclastic).

Two main clay mineral assemblages dominate in: (i) epiclastic units, in which pre-existing clay minerals (saponite, mica, talc, C/S mixed layers and chlorite) coexist with neoformed smectite (beidellite–montmorillonite); and (ii) pyroclastic and related paleosols, where smectite (beidellite–montmorillonite, saponite), zeolites and calcite of hydrothermal origin were formed.

Smectite of the epiclastic units show higher compositional variability compared to smectites in the pyroclastic rocks and in paleosols. Neoformed smectite (montmorillonite–beidellite) was also differentiated from pre-existing saponite by their primary textural features observed in SEM-HRTEM. Smectite formed in sedimentary environments is directly related to the different lithology of the bulk rock protolith. Mineralogical and chemical data also reveal that lacustrine and terrace Caldera de Taburiente deposits have the highest proportion of pre-existing clay minerals (saponite, corrensite, chlorite mica and talc) owing to a higher debris contribution from

Miocene volcanic basement rocks than in the fan delta sediments.

Smectite of the paleosols and the pyroclastic rocks has a uniform composition due to in situ transformation processes of volcanic debris. Moreover, hydrothermal fluids exerted a homogenizing effect on the mineralogy giving rise exclusively to smectite together with zeolites and calcite.

Acknowledgements

We would like to thank S. Morad for providing extremely helpful reviews of the manuscript and to A. Hernández-Pacheco for his constructive comments. We are also very grateful to M. Suárez and M. Besonen for the revision of the manuscript. We thank as well Dr K. A. W. Crook, Dr R. J. Merriman and an anonymous referee for their valuable discussions and helpful comments. Financial support was provided by CICYT, project BTE2000-0574-C03-02 (R. Marfil).

References

Abdel-Monem A, Watkins ND, Gast PW. Potassium–argon ages, volcanic stratigraphy, and geomagnetic polarity history of the Canary Islands: Tenerife, La Palma and Hierro. Am J Sci 1972;272:805–25.

Alt JC. Very low-grade hydrothermal metamorphism of basic igneous rocks. In: Frey M, Robinson D, editors. Low grade metamorphism. Oxford Blackwell Science; 1999. p. 169–201.

Álvarez-Ramis MC, Laamarti N, Vegas J. A preliminary palynological study of epiclastic deposits from "Caldera de Taburiente" La Palma island Canary archipelago, Spain. Plant Cell Biol Dev 2000;11:50–7.

Amouric M, Olives J, Dekayir A, El Maataoui M. Clay study in an altered basalt from Morocco. Proceedings of the 1st Latin American Clay Conference, Funchal, vol 1; 2000. p. 23–6.

Ancochea E, Hernán F, Cendrero A, Cantagrel JM, Fúster JM, Ibarrola E, et al. Constructive and destructive episodes in the building of a young Oceanic Island, La Palma, Canary Islands, and genesis of the Caldera de Taburiente. J Volcanol Geotherm Res 1994;60:243–62.

Aoudjit H, Robert M, Elsass F, Curmi P. Detailed study of smectite genesis in granitic saprolites by analytical electron microscopy. Clay Miner 1995;30:135–47.

Araña V, Ortiz R. The Canary Islands: tectonics, magmatism and geodynamic framework. In: Kampunzu AB, Lubala RT, editors. Magmatism in extensional structural settingsThe Phanerozoic African plate. Berlin: Springer-Verlag; 1991. p. 209–49.

Bargar KE, Beeson MH. Hydrothermal alteration in research drill hole Y-2, Lower Geyser Basin, Yellowstone National Park, Wyoming. Am Mineral 1981:473–90.

Beaufort D, Baronnet A, Lanson BB, Meunier A. Corrensite: a single phase or mixed-layer phyllosilicate in the saponite-to-chlorite conversion series? A case study of Sancerre couy deep drill hole (France). Am Mineral 1997;82:109–24.

Bird D, Schiffman P, Elders WA, Williams AE, McDowell SD. Calc-silicate mineralization in active geothermal systems. Econ Geol 1984;79:671–95.

Carracedo JC, Day SJ, Guillou H, Gravestock P. Later stages of volcanic evolution of La Palma, Canary Islands: rift evolution, giant landslides, and the genesis of the Caldera de Taburiente. Geol Soc Amer Bull 1999;111:755–68.

Cas RAF, Wright JV. Volcanic succession modern and ancient. London: Unwin Hyman; 1987. 528 pp.

Christidis GE, Scott PW, Marcopoulos T. Origin of the bentonite deposits of eastern Milos Aegean, Greece: geological, mineralogical and geochemical evidence. Clays Clay Miner 1995;43:63–77.

Cuevas J, Garralón A, Ramirez S, Leguey S. Hydrothermal alteration of a saponitic bentonite: mineral reactivity and evolution of surface properties. Clay Miner 2001;36:61–74.

De la Nuez, J. El complejo intrusivo subvolcánico de la Caldera de Taburiente, La Palma (Canarias). PhD Thesis, Ed. Univ. Complutense, Madrid, Spain; 1983.

Drief A, Nieto F, Sanchez-Navas A. Experimental clay-mineral formation from a subvolcanic rock by interaction with 1 M NaOH solution at room temperature. Clays Clay Miner 2001;49:92–106.

Ece ÖI, Çoban F, Güngör N, Suner F. Clay mineralogy and occurrence of ferrian smectites between serpentinite saprolites and basalts in Biga peninsula Northwest Turkey. Clays Clay Miner 1999;47:241–51.

Feraud, G. Datations des réseaux de dykes et de roches volcaniques sous-marines par les méthodes K–Ar et ^{40}Ar-^{39}. Utilisation des dykes comme marqueurs de paleocrontraintes, PhD Thesis, Univ. of Nice, France; 1981.

Fiore S, Huertas FJ, Huertas F, Linares J. Smectite formation in rhyolitic obsidian as inferred by microscopic (SEM-TEM-AEM) investigation. Clay Miner 2001;36:489–500.

Fisher RV, Schmincke HV. Pyroclastic rocks. Heidelberg: Springer-Verlag; 1984. 472 pp.

Grauby O, Petit S, Decarreau A, Baronnet A. The nontronite–saponitte series: an experimental approach. Eur J Mineral 1994;6:99–112.

Hernández-Pacheco A. Nota previa sobre el Complejo Basal de la Isla de La Palma (Canarias). Estud Geol 1971;27:255–265.

Hernández-Pacheco A, Fernández Santín S. Las formaciones volcánicas submarinas de la Caldera de Taburiente en La Palma (Canarias) y sus transformaciones metasomáticas. Proceedings of the Symposium on Andean and Antartic Volcanology Problems. Santiago, Chile; 1974. p. 98–111.

Huertas FJ, Cuadros J, Huertas F, Linares F. Experimental study of the hidroternal formation of smectite in the beidellite–saponite series. Am J Sci 2000;300:504–27.

Inoue A. Formation of clay minerals in hydrothermal environments. In: Velde B, editor. Origin and mineralogy of clays. Springer; 1995. 268–329.

Kloprogge JT, Komameni S, Amonette JE. Synthesis of smectite clay minerals: a critical review. Clays Clay Miner 1999;47: 529–54.

Kristmannsdottir H, Tomasson J. Zeolite zones in geothermal areas in Iceland. In: Sand LB, Mumpton FA, editors. Natural zeolites, occurrences, properties, use. New York: Pergamon; 1978. p. 277–84.

Kühnel RA, Van Der Gaast SJ. Inhomogeneous clay mineral formation in volcanic rocks from Gran Canaria, Spain: preliminary results. Proceedings of the 1st Latin American Clay Conference, Funchal, vol. 1; 2000. 15–26.

Laverne C, Belarouchi A, Honnorez J. Alteration mineralogy and chemistry of the upper oceanic crust from Hole 896A, Costa Rica rift. In: Alt JC, et al, editors. Proc ODP, Sci Results, vol. 148. College Station, TX: Ocean Drilling Program; 1996. p. 151–70.

Minato H. Formation mechanisms of clay minerals from andesitic volcanic materials by reactions of weathering processes. Proceedings of the 1st Latin American Clay Conference, Funchal, vol. 1; 2000. p. 48–58.

Mizota Ch, Faure K. Hydrothermal origin of smectite in volcanic ash. Clays Clay Miner 1998;46:178–82.

Newman ACD, Brown G. The chemical constitution of clays. In: Newman ACD, editor. Chemistry of clays and clay minerals. Mineralogical Society Monograph, vol. 6. London: Longman Scientific and Technical Mineralogical Society; 1987. p. 1–129.

Pevear DR, Dethier DP, Frank D. Clay minerals in the 1980 deposits from Mount St Helens. Clays Clay Miner 1982;30:241–52.

Ramirez S, Vigil R, Cuevas J, Leguey S. Zeolite and smectite crystallization on a bentonite matrix in an hydrothermal alkaline environment. Proceedings of the 2nd Mediterranean Clay Meeting, Aveiro, vol. 2; 1998. p. 87–92.

Roberson HE, Reynolds RC, Jenkins DM. Hydrothermal synthesis of corrensite: a study of the transformation of saponite to corrensite. Clays and Clays Miner 1999;47:212–8.

Robinson D, Bevins RE, Rowbotham G. The characterization of mafic phyllosilicates in low-grade metabasalts from eastern North Greenland. Am Mineral 1993;78:377–90.

Schiffman P, Staudigel H. Hydrothermal alteration of a seamount complex on La Palma, Canary Island: implications for metamorphis in accreted terranes. Geology 1994;22:151–4.

Schiffman P, Staudigel H. The smectite to chlorite transition in a fossil seamount hydrothermal system: the Basement Complex of La Palma, Canary Islands. J Metamorph Geol 1995;13:487–98.

Shau YH, Peacor DR. Phyllosilicates in hydrotherally altered basalts from DSDP Hole 504B, Leg 83-a TEM and AEM study. Contrib Mineral Petrol 1992;112:119–33.

Shau Y-H, Peacor DR, Essense SE. Corrensite and mixed-layer chlorite/corrensite in metabasalt from northern Taiwan: TEM/ AEM, EMPA, XRD and optical studies. Contrib Mineral Petrol 1990;105:123–42.

Staudigel H, Féraud G, Giannerini G. The history of intrusive activity on the island of La Pahna (Canary Islands). J Volcanol Geotherm Res 1986;27:299–322.

Tessier, D., 1984. Etude experimentale de ´organisation des matériaux argileux, PhD Théses. INRA, Paris. 361 pp.

Vegas J, García-Romero E, Marfil R. Procesos de transformación y neoformación de esmectitas en los materiales volcanoclásticos de la isla de La Palma (Canarias). Geogaceta 1999a;25:207–10.

Vegas J, Hernández-Pacheco A, Marfil R. Los depósitos volcanoclásticos de la isla de La Palma (Canarias): su relación con la evolución de las Calderas de Taburiente y Cumbre Nueva. Bol Geol Min 1999b;110:135–58.